Journal of Applied Polymer Science

# Preparation and Properties of Hydrophobic Poly(vinylidene fluoride)–$SiO_2$ Mixed Matrix Membranes for Dissolved Oxygen Removal from Water

**Ting Li, Ping Yu, Yunbai Luo**
College of Chemistry and Molecular Sciences, Wuhan University, Wuhan 430072, Hubei, People's Republic of China
Correspondence to: P. Yu (E-mail: yuping@whu.edu.cn)

**ABSTRACT:** The application of the membrane method for removing dissolved oxygen (DO) from water on the laboratory scale was studied. Flat mixed matrix membranes were composed of poly(vinylidene fluoride) (PVDF) and hydrophobic nanosilica particles, which were used to improve the DO removal process. The $SiO_2$ particles were modified by a silane coupling agent and examined by Fourier transform infrared spectroscopy. It was shown that the surface of the $SiO_2$ particles was bonded to hydrophobic long-chain alkane groups through chemical bonding. The effects of adding $SiO_2$ particles on the membrane properties and morphology were examined. The results show that the porosity and pore size of the membrane were affected by the introduction of $SiO_2$ particles, and the cross-sectional morphology of the PVDF composite membranes changed from fingerlike macrovoids to a spongelike structure. The membrane performance of DO removal was evaluated through the membrane unit by a vacuum degassing process. It was found that the $SiO_2$/PVDF hybrid membranes effectively improved the oxygen removal efficiency compared with the original PVDF membranes. The maximum permeation flux was obtained when the loading amount was 2.5 wt %. The effect of the downstream vacuum level was also investigated. The experimental results show that the $SiO_2$/PVDF hybrid membranes had superior performances and could be an alternative membrane for removing DO from water. © 2014 Wiley Periodicals, Inc. J. Appl. Polym. Sci. **2014**, *131*, 40430.

**KEYWORDS:** membranes; properties and characterization; nanoparticles; nanowires and nanocrystals

Received 31 October 2013; accepted 13 January 2014
**DOI: 10.1002/app.40430**

## INTRODUCTION

The removal of dissolved oxygen (DO) from water is one of the primary processes applied in various industries, including the food, power plant, semiconductor manufacturing, pharmaceutical, and biotechnology industries.[1–3] In the power industry, for example, the presence of DO in the boiler feed water can result in the corrosion of the boilers or steel pipes and can cause tube explosion. In the semiconductor industry, the removal of DO is necessary for preventing the formation of a native oxide layer on the surface of silicon wafers during the cleaning process.[2] This native oxide layer may impede the development of high-performance processes. There are several effective methods for removing DO from water by physical methods, such as thermal or vacuum degassing processes and chemical reduction processes with hydrazine or sodium sulfite.[4,5] Physical methods have the inherent drawbacks of being costly and bulky. Chemical methods are undesirable because of the toxicity of hydrazine, and the increase in the solid content in water through the addition of sodium sulfite needs a further process of ion exchange.

Nowadays, membrane separation technology is rapidly emerging as an energy efficient and environmentally friendly technology. Progress in membrane modules has provided an attractive alternative for dissolved gases removal in water.[6–8] Membrane degassing is a new type of liquid–gas membrane separation processes that mergers membrane separation and gas removal technologies.[9–13] In this process, the gas components diffuse through the membrane, and the membrane is used as a barrier between the gas phase and the liquid phase. The membrane process provides many advantages, such as a fast mass transfer efficiency, large surface area per unit volume, and tight modular construction, in comparison to the traditional physical methods. Hydrophobic membranes are often used for DO removal from water. The hydrophobicity of the membrane has a large tension, which prevents water from penetrating into the membrane pores. Furthermore, the characteristics of hydrophobic and microporous membranes can promote mass transfer between phases, and less mass transfer resistance is obtained.[14] Poly(vinylidene fluoride) (PVDF) has emerged as an appropriate

membrane material for deoxygenation processes because of its good hydrophobicity. Compared to other commercial hydrophobic polymeric materials, such as polypropylene and polytetrafluoroethylene, PVDF can be easily dissolved in organic solvents, and a membrane with porous and asymmetric structure can be produced via a phase-inversion method, which may provide a controllable morphology and porosity of membranes.

The blending of inorganic nanoparticles with a polymer dope solution is of considerable interest in the preparation of mixed matrix membranes (MMMs), which can be widely applied in ultrafiltration, desalination, pervaporation, gas separation, and other processes.[15–21] Nanoparticles have continued to achieve higher permeability and have improved the properties of polymers to a certain extent because of their large specific surface areas, small sizes, and strong surface energies.[16,22] Compared to the original polymeric membranes, a significant improvement in the membrane performance is expected for MMMs. Inorganic particles, including $SiO_2$, $TiO_2$, $ZrO_2$, $Al_2O_3$, and $Fe_3O_4$, have been introduced into PVDF membranes.[23–29] Among them, $SiO_2$ has been found to be the most widely used; it has chemical resistance and good compatibility with the organic solvents used to prepare the PVDF solution. The investigation of novel polymeric–inorganic composite membranes for ultrafiltration was reported by Bottino et al.,[30] who discovered an increase in permeation flux when they added silica particles into the porous matrix of PVDF. Arthanareeswaran et al.[31] prepared Cellulose acetate/$SiO_2$ hybrid membranes by a phase-inversion processes. They observed that the pore radius, porosity, and fouling resistance of the membranes increased with increasing $SiO_2$ content. Some studies have also proven that the introduction of silica into organic polymers can enhance the physical stability and separation performance of membranes.[32,33]

Over the past several years, research in membrane technology for DO removal from water has mainly focused on the improvement of design membrane module and devices; the feasibility of fabricating high-performance membranes for the deoxygenation process has been studied less.[34–36] The objective of this study was to develop highly permeable PVDF matrix membranes for the removal of DO. In this study, a hydrophobic organic–inorganic composite membrane was prepared by the incorporation of nano-$SiO_2$ into the PVDF solution via a phase-inversion method for DO removal applications. To maintain the hydrophobicity of the PVDF MMMs, the $SiO_2$ surface was grafted with *n*-dodecyl chains by a silane coupling agent, dodecyltrimethoxysilane (DTMS). The structures and properties of the PVDF composite membranes were characterized, and the degassing performance in a laboratory-scale membrane degassing system for DO removal from water under vacuum conditions was studied.

## EXPERIMENTAL

### Materials

PVDF resin FR-904 (number-average molecular weight = 380,000) was purchased from Shanghai New Materials Co., Ltd. DTMS was used as a silane coupling agent, and nano-$SiO_2$ (particle size = 7 nm) were obtained by WD Silicone New Material Co., Ltd. *N,N*-Dimethylacetamide (DMAc), ethanol, and isopropyl alcohol were obtained as analytical reagents from Sinopharm Chemical Reagent Co., Ltd. Deionized water was used in all of the experiments.

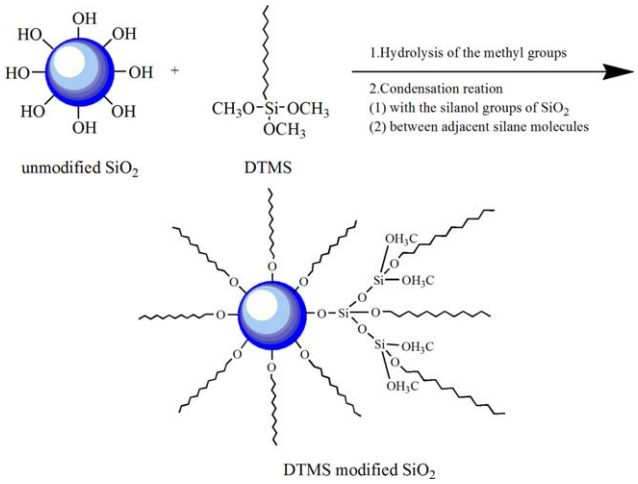


**Figure 1.** Schematic representation of the chemical modification of the $SiO_2$ surface with silane coupling. [Color figure can be viewed in the online issue, which is available at wileyonlinelibrary.com.]

### Surface Modification of the $SiO_2$ Particles

The surfaces of nanosilica particles were covered by silanol groups. Chemical treatment of the nanoparticle surface was necessary to preserve the hydrophobicity of the PVDF hybrid membranes. The surface modification reaction is shown in Figure 1. When hydrolysis and condensation reactions occurred between the DTMS and $SiO_2$ surface, the silanol groups of the $SiO_2$ surfaces decreased through the condensation reaction and made the surface hydrophobic.[37] Silane-modified nano-$SiO_2$ particles were prepared as follows: $SiO_2$ was added in the DTMS ethanol solution (pH 4–5, adjusted by acetic acid), and the reaction mixture was stirred at 323 K for 12 h. After the treatment, the $SiO_2$ particles were centrifuged and washed with ethanol several times until no silane coupling agent was detected in the filtrate. The surface-modified $SiO_2$ particles were finally obtained by drying at 323 K for 24 h in a vacuum.

### Preparation of PVDF MMMs

Nano-$SiO_2$ was incorporated into the PVDF matrix to form MMMs by a phase-inversion method. A predetermined amount of $SiO_2$ particles was added to the DMAc solvent, and the mixture was sonicated for 30 min to ensure homogeneous spreading of the nanoparticles. Then, PVDF was added to the mixture and dissolved under stirring at 333 K for 12 h. Before casting, the solution was kept in a vacuum oven to remove the gas bubbles. The solution was cast uniformly onto a smooth glass plate by a hand-casting blade and was then immersed in a water bath three times to remove the residual solvents. The membranes were treated further by immersion in an ethanol aqueous solution for 24 h and were then dried at room temperature to minimize membrane deformation and pore collapse. The treatment was identical to that of the pristine membrane. Six different weight concentrations (0, 1, 2, 2.5, 3, and 4 wt % by weight of

the solution) of modified $SiO_2$ added to the polymer dopes consisting of PVDF (15 wt % by weight of the solution), and DMAc (85 wt % by weight of the solution) were prepared. These were designated as PVDF-0, PVDF-1, PVDF-2, PVDF-3, PVDF-4, and PVDF-5, respectively.

### Characterization of $SiO_2$ Particles and Membranes

**Fourier Transform Infrared (FTIR) Analysis.** FTIR spectroscopy was used to analyze the $SiO_2$ particles and whether the surface modification had actually reacted; the instrument was a Nicolet AVATAR 360 FTIR spectrophotometer used in the scanning range 4000–500 $cm^{-1}$.

**Morphological Analysis.** Scanning electron microscopy (SEM) was used to observe the cross-sectional morphology of the pure PVDF and $SiO_2$/PVDF hybrid membranes. The membranes were immersed in liquid nitrogen and fractured, and then, the fractured section was sputter-coated with a thin film of gold. The membranes were mounted on brass plates with double-sided conductive adhesive tape in a lateral position. The cross section of the membranes was obtained with SEM (FEI Quanta 200, Holland).

**Hydrophobicity, Porosity, and Pore Size Measurements.** The contact angle ($\theta$; °) was measured to estimate the hydrophobicity of the membrane with a DSA100 instrument (Kruss, Germany).

The membrane porosity ($\varepsilon$; %) was measured with a dry–wet weight method. The porosity was measured with the following steps: (1) immersion of the dry membranes in isopropyl alcohol for 1 h, (2) weighing of the membranes before and after the absorption of isopropyl alcohol, and (3) calculation of the porosity of the membranes with eq. (1):[26]

$$\varepsilon = \frac{(W_1 - W_2)/\rho_i}{(W_1 - W_2)/\rho_i + W_2/\rho_{PVDF}} \times 100\% \quad (1)$$

where $W_1$ is the weight of the wet membrane (g), $W_2$ is the weight of the dry membrane (g), $\rho_i$ is the density of isopropyl alcohol ($g/m^3$), and $\rho_{PVDF}$ is the density of the dry-state membrane ($g/m^3$).

The mean pore radius ($r_m$; m) was characterized by the filtration velocity method. It was calculated by the following equation revised from the Guerout–Elford–Ferry equation according to eq. (2):[38]

$$r_m = \sqrt{\frac{(2.9 - 1.75\varepsilon) \times 8\mu l Q_t}{\varepsilon \times A \times \Delta P}} \quad (2)$$

where $\mu$ is the water viscosity (Pa s), $l$ is the membrane thickness (m), $Q_t$ is the volume of the permeate water per unit time ($m^3/s$), $A$ is the effective area of the membrane ($m^2$), and $\Delta P$ is the operational pressure (Pa).

The maximum pore radius ($r_{max}$; m) was determined by the bubble-point method. It was based on the measurement of the pressure needed to blow nitrogen through a liquid-filled membrane. The membrane was immersed in ethanol, and pressure was applied to the membrane base. The maximum pore radius could be calculated according to the Young–Laplace equation by eq. (3):[9]

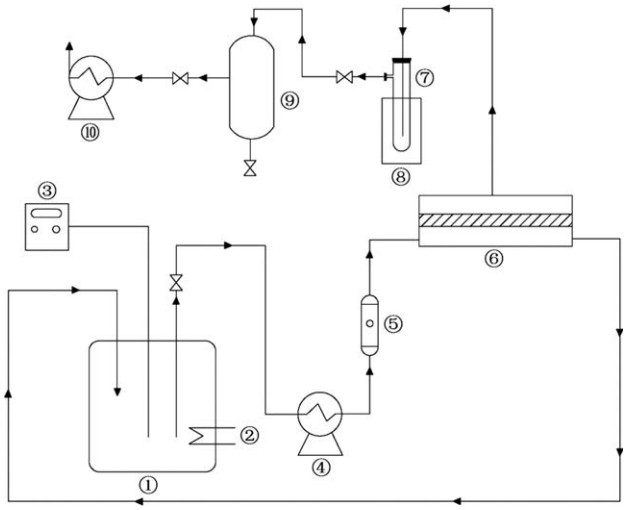


**Figure 2.** Schematic diagram of the experimental apparatus for DO removal: (1) feed tank, (2) heating unit, (3) DO meter, (4) flow control pump, (5) rotameter, (6) membrane cell, (7) collecting bottle, (8) liquid nitrogen cold trap, (9) buffer vessel, and (10) vacuum pump.

$$r_{max} = \frac{2\sigma\cos\theta}{P} \quad (3)$$

where $\sigma$ is the surface tension of ethanol (N/m), $\theta$ is the contact angle of ethanol with the membrane (°), and $P$ is the minimum bubble-point pressure (Pa).

All of the obtained values were the average of five different measurements at various positions of the sample.

### Performance of the Membrane in DO Removal

The scheme of the experimental setup used for the deoxygenation process is shown in Figure 2. The membrane, with an effective area of 51.35 $cm^2$ in contact with the feed water, was supported by a porous, stainless flat-sheet membrane cell. The volume of the feed tank was 5.2 L, and the feed tank was maintained at a constant temperature by a thermocouple with accuracies of ±0.1 K. The feed water saturated with air was continuously circulated into the membrane cell with a flow control pump, and the flow rates were measured with a rotameter on the upstream side of the membrane cell while a vacuum was exerted on the downstream side of the membrane cell with a vacuum pump. The water vapor permeating through the membrane was collected in a liquid nitrogen trap for condensation. The microporous PVDF membrane had small pores, which allowed the DO to pass through the membrane under vacuum conditions, whereas the hydrophobic properties restrained water from passing through the pores. The membrane had a high resistance to water but offered little resistance to gases. As a result, the gases were removed from the water stream, and the DO concentration in the feed water decreased.

The DO concentration in the feed water was continuously measured with a DO meter (HQ30d, HACH Co.). Because the DO removal experiment in a sealed system was studied, the weight of removed oxygen could be calculated by the change in the DO concentrations in the feed water. The permeation fluxes

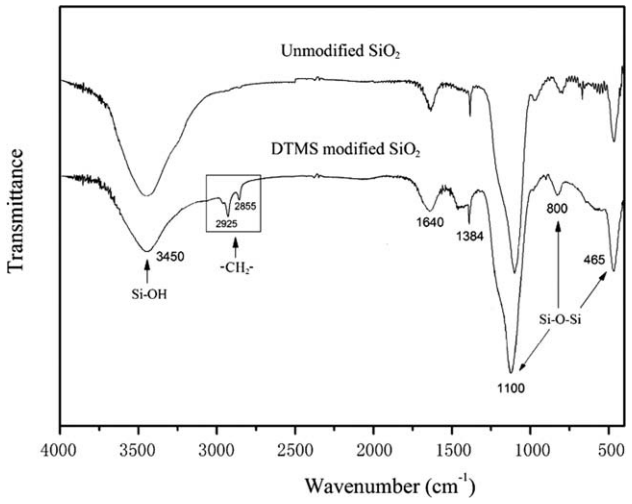


**Figure 3.** FTIR spectra of the unmodified $SiO_2$ particles and DTMS-modified $SiO_2$ particles.

($g/m^2$ h) of oxygen ($J_o$) and water ($J_w$), and the oxygen removal efficiency ($\eta$) were calculated with the following equations:

$$J_o\,(g/m^2\,h) = \frac{Q_o}{A \times \Delta T} \tag{4}$$

$$J_w\,(g/m^2\,h) = \frac{Q_w}{A \times \Delta T} \tag{5}$$

$$\eta = \frac{C_{in} - C_{out}}{C_{in}} \times 100\% \tag{6}$$

where $Q_o$ is the weight of oxygen removal from water (g), $Q_w$ is the weight of water congealed in the liquid nitrogen cold trap (g), $\Delta T$ is the predetermined duration of time for the DO removal process (h), $A$ is the effective membrane area ($m^2$), and $C_{in}$ and $C_{out}$ are the oxygen concentrations in the feed water at beginning and at the end, respectively.

All of the experiments were repeated several times to ensure the reproducibility, and a maximum fluctuation of 2% was obtained.

## RESULTS AND DISCUSSION

**Characterization of the $SiO_2$ Particles and Hybrid Membranes FTIR Spectroscopy.** Figure 3 shows the FTIR spectrum of $SiO_2$ before and after modification with DTMS. As shown in Figure 3, the peak that was observed at 3450 $cm^{-1}$ in the spectrum was attributed to terminal silanol groups. However, in the spectra of the modified $SiO_2$, the decrease in the peak intensity at 3450 $cm^{-1}$ was significant; this suggested that the condensation reaction between DTMS and $SiO_2$ occurred on the outer surface of the $SiO_2$ particles. Furthermore, compared with the unmodified $SiO_2$ particles, a new broad absorption band around 2800–3000 $cm^{-1}$ was found in the spectra of the DTMS-modified $SiO_2$, the peak at 2960 $cm^{-1}$ was the asymmetric stretching vibration of —$CH_3$ groups, and the peaks located at 2925 and 2855 $cm^{-1}$ were the asymmetric and symmetric stretching vibrations of the —$CH_2$— groups. These peaks were from long-chain alkane groups in DTMS.[39] This confirmed that DTMS was successfully grafted onto the external surface of the $SiO_2$ particles. The figure shows that the characteristic peaks of $SiO_2$ at 465, 800, and 1100 $cm^{-1}$ were almost the same for both the unmodified and DTMS-modified $SiO_2$; this indicated that the $SiO_2$ structure was not changed by the modification.[40]

**Morphological Analysis.** The cross-sectional morphologies of the PVDF MMMs are shown in Figure 4. The figures showed that the PVDF membrane prepared by phase-inversion methods produced an asymmetric structure with a fingerlike macrovoids layer and a spongelike microporous layer, which offered much less mass-transfer resistance. Compared with the original PVDF membrane, more spongelike micropores were observed in the PVDF MMMs, and the transmutation of fingerlike macrovoids became obvious with increasing $SiO_2$ concentration. This could be explained by the kinetic rate of solvent–nonsolvent exchange in the phase-inversion process to form an asymmetric structure.[41] When the $SiO_2$ concentration was high, the viscosity of the casting solution increased simultaneously; the rate of water intrusion into the polymer dope decreased, and this led to slower demixing in the coagulation bath and resulted in a transmutative fingerlike macrovoid layer and more spongelike micropores, as shown in Figure 4(A–C). The larger spongelike pore network containing a large volume of air might provide less resistance for oxygen transport through the PVDF membrane.[14] SEM images of the membrane showed that the $SiO_2$ particles were distributed uniformly throughout the polymer matrix at lower concentrations [Figure 4(b)] and the appearance of particle agglomeration at higher $SiO_2$ concentration [Figure 4(c)]. This phenomenon may due to the precipitation of the particles during the mixing operation, the inorganic phases, and the polymer phases, which resulted in inhomogeneity. Therefore, the aggregation of $SiO_2$ particles in the PVDF MMMs was even more serious when the $SiO_2$ loading was very high. A similar conclusion was reached by Huang et al.[43] These changes indicated that the cross-sectional morphology of the membranes was influenced by the addition of inorganic particles.

**Contact Angles, Porosity, and Pore Sizes of the Membranes.** The microporous membrane acts as a barrier in the deoxygenation process. The membrane properties, such as the hydrophobicity, porosity, and pore size play an important role and influence the degassing performance. The contact angle, porosity, and pore size of the PVDF MMMs are listed in Table I. In the degassing process, the membranes with a high hydrophobicity could resist wetting. The contact angle is an important parameter for measuring the surface hydrophobicity. It was shown that the contact angle showed a slight increase with different $SiO_2$ amounts. Because the surfaces of the virgin silica particles that were covered by silanol groups were hydrophilic, it was confirmed that the chemical treatment of the nanoparticle surface was effective and necessary, and the surface hydrophobicity of the PVDF membranes was maintained by the addition of modified $SiO_2$. Furthermore, the porosity of the membranes first increased and then decreased with increasing $SiO_2$ loading. This could have been due to the interfacial stress relaxation between the polymer and the inorganic phase during the phase-inversion process, which increased the amount of micropores on the solid–liquid interface at lower filling amounts. However, the particles blocked the pores partially and decreased the porosity when the $SiO_2$ concentration was high.[16]

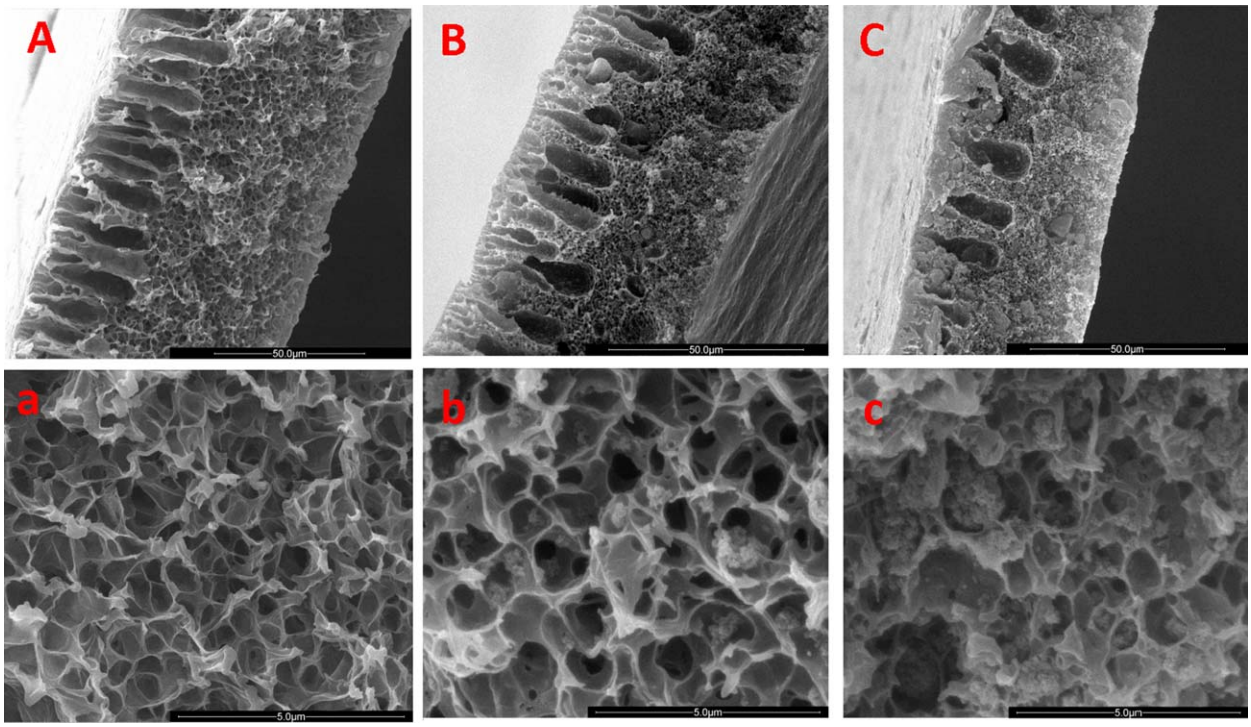


**Figure 4.** Cross-sectional SEM images of (A,a) PVDF-0, (B,b) PVDF-3, and (C,c) PVDF-5 hybrid membranes. [Color figure can be viewed in the online issue, which is available at wileyonlinelibrary.com.]

This phenomenon was also confirmed by the cross-sectional SEM images shown in Figure 4. The trend of the changes in the mean pore size and the maximum pore size with different $SiO_2$ concentrations indicated that a higher $SiO_2$ concentration resulted in an increase in the membrane pore size. The investigation of Cellulose acetate/$SiO_2$ hybrid membranes by Arthanareeswaran et al.[31] followed a similar trend, in which the blending of the $SiO_2$ particles was an effective way to increase the porosity and pore radius of the membranes. The mean pore radius and maximum pore radius were changed greatly in comparison with the pure PVDF membrane.

### Membrane Deoxygenation Performance

**Effect of the $SiO_2$ Content on the Hybrid Membranes.** The performances of the PVDF MMMs on the removal of DO were evaluated and are shown in Figure 5. The DO concentration in the feed water was kept at 9 mg/L, and the experiments had a duration of 1 h. As shown in Figure 5(a,b), the PVDF MMMs improved the oxygen removal efficiency and permeation flux effectively compared with the original membrane (PVDF-0). The oxygen permeation flux of the membranes showed an initial rise with when the $SiO_2$ concentration was increased to 2.5 wt % (PVDF-3); then, it decreased by a small amount when the $SiO_2$ concentration was increased to 4 wt % (PVDF-5).

The PVDF-3 membrane displayed ideal comprehensive performances in the oxygen removal efficiency and the oxygen permeation flux. As shown in Figure 5(b), the oxygen permeation flux of PVDF-3 was 2298.73 mg/$m^2$ h; this was much higher than that of the original PVDF membrane (1488.61 mg/$m^2$h). A higher $SiO_2$ content in the membranes resulted in a greater enhancement of the degassing performance. The facts were attributed to the introduction of $SiO_2$ particles to the PVDF membrane; this made a more compact network and changed the trend of crystallinity. The presence of the inorganic phase served to confine the molecular motions of the polymer chains, and the addition of $SiO_2$ had a large influence on the membrane structure and properties (as shown in Figure 4 and Table I). This provided more micropores and a greater polymer/$SiO_2$ interfacial area and offered space for oxygen molecules to pass through the membranes. Limited

**Table I.** Membrane Contact Angles, Porosity, and Pore Sizes of the Membranes

| Membrane | Contact angle (°) | Porosity (%) | Mean pore radius (μm) | Maximum pore radius (μm) |
|---|---|---|---|---|
| PVDF-0 | 98.2 ± 0.5 | 80.5 ± 1.5 | 0.043 ± 0.003 | 0.125 ± 0.009 |
| PVDF-1 | 99.1 ± 0.4 | 81.3 ± 1.8 | 0.048 ± 0.002 | 0.131 ± 0.011 |
| PVDF-2 | 100.8 ± 0.4 | 82.7 ± 1.6 | 0.054 ± 0.004 | 0.137 ± 0.012 |
| PVDF-3 | 101.4 ± 0.6 | 83.8 ± 1.3 | 0.057 ± 0.006 | 0.144 ± 0.017 |
| PVDF-4 | 102.2 ± 0.5 | 83.4 ± 1.5 | 0.053 ± 0.003 | 0.134 ± 0.008 |
| PVDF-5 | 102.7 ± 0.6 | 82.3 ± 1.1 | 0.046 ± 0.005 | 0.129 ± 0.009 |

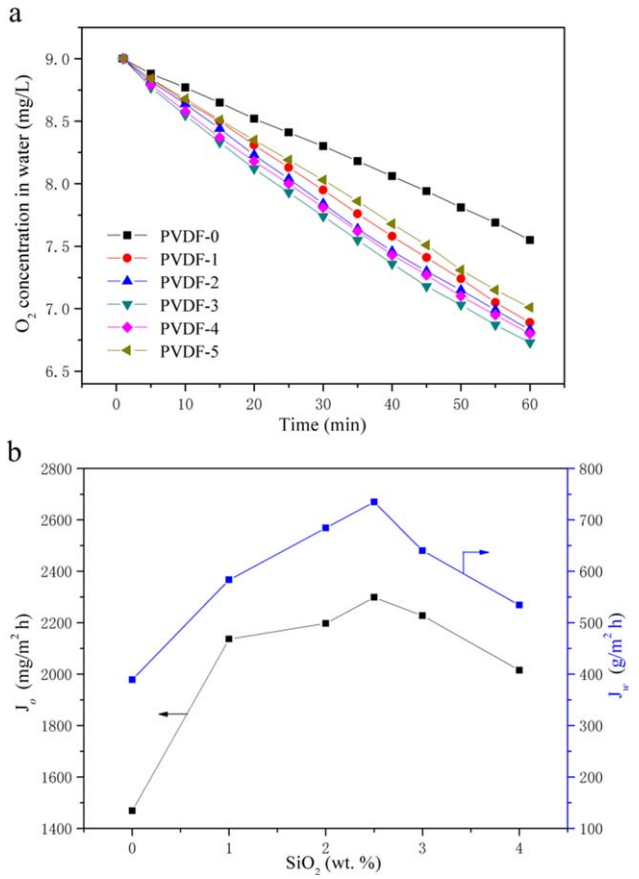


**Figure 5.** (a) Oxygen removal efficiency and (b) permeation flux of oxygen and water with different $SiO_2$ concentrations. [Color figure can be viewed in the online issue, which is available at wileyonlinelibrary.com.]

molecular motions and a favorable increase of the micropore network for the hydrophobic membrane could potentially result in a higher permeability of oxygen and more oxygen transport through the membrane.[31] The oxygen permeation flux decreased when the $SiO_2$ loading was greater than 2.5 wt %; this was probably due to the uneven dispersal and the appearance of particle agglomeration at higher $SiO_2$ concentrations. Some researchers have come to similar conclusions, in which the separation properties were improved effectively by the dispersal of inorganic particles uniformly into the polymer membrane.[28]

In addition to the better hydrophobicity and porosity (as shown in Table I) of the PVDF-3 membrane, the appropriate pore structure (as shown in Figure 4) and excellent deoxygenation performances (as shown in Figure 5) made it a good selection for the DO removal process. Indeed, the high porosity of the membrane provided larger liquid–gas contact areas and less resistance for oxygen transport for the degassing process. Therefore, by controlling the $SiO_2$ concentration of the PVDF MMMs, an improved membrane could be obtained to enhance the oxygen removal efficiency.

The influence on the water permeation flux is shown in Figure 5(b). The results show that the change tendency of the water permeation flux was basically the same as that of the oxygen permeation flux, which showed the maximum value at 2.5 wt %. The DO removal process was operated under vacuum conditions; in general, water can enter into the porous membrane either as a liquid or a vapor. Because of the PVDF membrane was hydrophobic and the pore size of the membranes was very small, water was prevented from entering the PVDF membrane, and water vapor could condense in the micropores. In our study, it was found that the weight of water vapor permeating through the membrane was relatively small and could be considered to be negligible compared with the total weight of the feed water. Moreover, the existence of water vapor in the

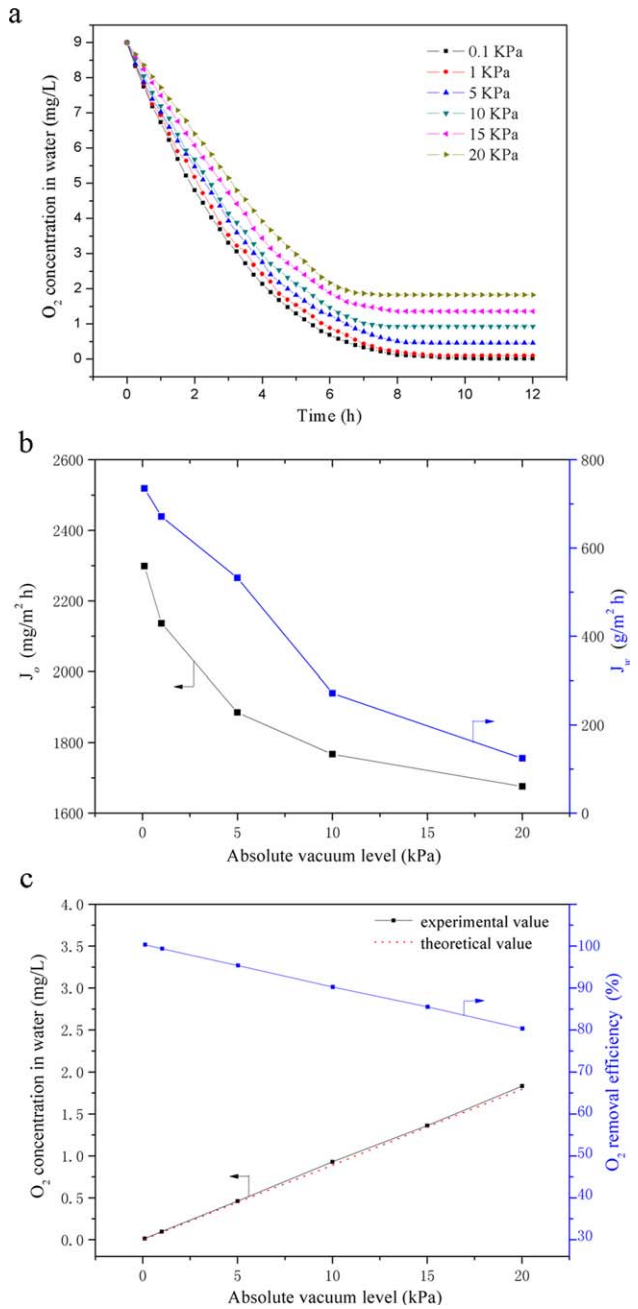


**Figure 6.** (a) Oxygen removal efficiency, (b) permeation flux of oxygen and water, and (c) experimental and theoretical values of the DO concentration with different operating vacuum levels. [Color figure can be viewed in the online issue, which is available at wileyonlinelibrary.com.]

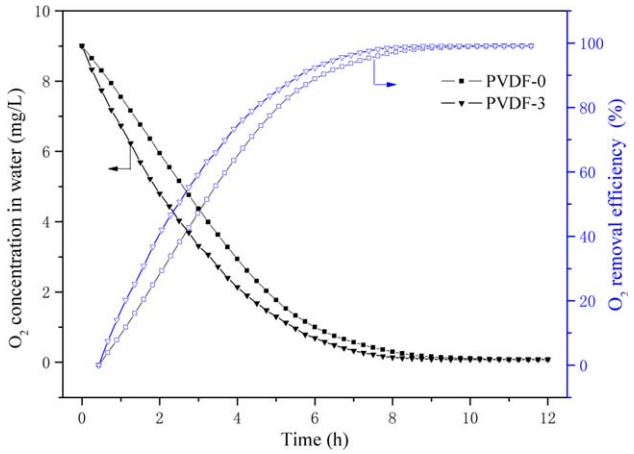


**Figure 7.** Effect of the long-term operating time with PVDF-0 and PVDF-3. [Color figure can be viewed in the online issue, which is available at wileyonlinelibrary.com.]

gas stream resulted in a lower oxygen partial pressure and enhanced the driving force for DO removal in a certain range. This may suggest that the small permeation of water vapor was conducive to the degassing process.

**Effect of the Operating Vacuum.** The operating vacuum level is an important factor in the degassing process. The oxygen removal performances were explored by both theoretical and experimental studies and are shown in Figure 6. Figure 6(a,b) shows the influence of the DO removal efficiency and the permeation fluxes with different operating vacuums. When the vacuum level in terms of absolute pressure was increased from 100 Pa to 20 kPa, both the oxygen removal efficiency and the permeation flux decreased because of the decreasing driving force for oxygen removal in water. The vacuum caused a deep drop on the oxygen partial pressure between the two sides of the membrane; this provided the driving force for oxygen removal. The vacuum resulted in a reduction in the solubility of oxygen in water and could impel the oxygen to move out until the balance was reached.[4] The decrease in the oxygen concentration was more significant in the first 4 h; this showed that a higher driving force was available at the beginning. The final concentration of DO in water was in direct proportion to the oxygen partial pressure on the interface of oxygen and water according to Henry's law. Figure 6(c) indicated that the theoretical final oxygen concentrations coincided with the experimental results well. When the vacuum level was kept at 100 Pa, a DO removal efficiency of more than 99.8% was achieved. Therefore, it should be possible to operate at a moderately low absolute pressure, and the higher driving force will provide a more efficient operation for separation.

**Long-Term Experiment.** To investigate the efficiency and performance for industrial applications of vacuum degassing with the membrane process, the membrane samples PVDF-0 and PVDF-3 were tested for oxygen removal in water. Figure 7 shows the influence of the operation time on the original PVDF and PVDF-3 for a long duration while the absolute vacuum level was kept at 100 Pa. The concentration of DO was 9 mg/L in the feed water. The results show that the final DO concentrations of PVDF-0 and PVDF-3 were kept the same under the long-term treatment with a decrease in the same DO concentration of 15 ppb. However, the equilibrium time of PVDF-3 was shorter than that of PVDF-0. A concentration gradient was created across the membrane under vacuum conditions, and the final equilibrium concentration of DO depended on the oxygen partial pressure on the interface of oxygen and water. The membrane only acted as a barrier and did not directly provide the selectivity in the degassing process. The final concentration of DO was determined by the operating vacuum. The PVDF MMMs were expected to have a higher degassing performance and lower operating costs, and the introduction of $SiO_2$ to the membranes was more productive and efficient in the long term.

## CONCLUSIONS

In this study, we developed a new type of PVDF MMM containing surface-modified nano-$SiO_2$ particles. The surfaces of nano-$SiO_2$ were modified by a silane coupling agent containing long-chain alkane groups to maintain the hydrophobicity of the hybrid membranes. The influence of the membrane morphology, contact angle, porosity, and pore size were examined, and the results indicate that the introduction of the $SiO_2$ particles affected the morphologies and properties significantly. The effect of the hybrid membranes on the DO removal experiment was investigated. As compared with the original PVDF membranes, the hybrid membranes improved the oxygen removal efficiency effectively, and the maximum permeation flux was obtained when the $SiO_2$ loading was 2.5 wt %. In the degassing process, the membrane acted only as a barrier between the two phases, and the DO removal efficiency was highly dependent on the membrane properties and structure. Therefore, by controlling the $SiO_2$ concentration in the PVDF MMMs, we achieved an improved structure of the PVDF membranes to enhance the DO removal efficiency. The DO removal performance of the PVDF MMMs increased with increasing operating vacuum. The vacuum membrane degassing is a very suitable method for removing DO from water and DO levels of 15 ppb could be achieved by long-term operation. The results show that this kind of composite membrane could efficiently remove DO, and it is expected to be a high-performance separation membrane. On the premise of the development of highly permeable PVDF matrix membranes, future research on the design of hollow-fiber membrane modules and a pilot-scale study will be widely developed and improved for practical applications. Because of the practical application process, a major drawback of membrane methods (or the physical methods) is that the lack of a driving force makes it hard to reach very low concentrations (e.g., $<$10 ppb). The required DO concentration in water had different levels for various applications. Membrane degassing is very effective and competitive in these less demanding applications when the requirements for DO in water are very critical, for example, in the semiconductor industry, where the requirements are often as low as 1 ppb. DO can be removed from water with a combination system of both a membrane technique and other methods. Hence, we concluded that a novel

oxygen removal membrane was obtained that had good potential to improve the membrane performance in industrial degassing applications.

## ACKNOWLEDGMENTS

This work was supported by the Plan of the National Science and Technology Support Program (contract grant number 2012BAC02B03) and the Fundamental Research Funds for the Central Universities of China (awards 2012203020213 and 201120302020012). The authors thank WD Silicone New Material Co., Ltd., for providing the silane coupling agent and nano-$SiO_2$ used in this study.

## REFERENCES

1. Ito, A.; Yamagiwa, K.; Tamura, M.; Furusawa, M. *J. Membr. Sci.* **1998**, *145*, 111.
2. Yagi, Y.; Imaoka, T.; Ksama, Y.; Ohmi, T. *IEEE Trans. Semicond. Manuf.* **1992**, *5*, 121.
3. Tan, X.; Li, K. *Chem. Eng. Sci.* **2000**, *55*, 1213.
4. Landman, M. J.; Van den Heuvel, M. R. *Water Res.* **2003**, *37*, 4337.
5. Moon, J. S.; Park, K. K.; Kim, J. H.; Seo, G. *Appl. Catal. A* **2000**, *201*, 81.
6. Atwater, J. E.; Akse, J. R. *J. Membr. Sci.* **2007**, *301*, 76.
7. Peng, Z. G.; Lee, S. H.; Zhou, T.; Shieh, J. J.; Chung, T. S. *Desalination* **2008**, *234*, 316.
8. Criscuoli, A.; Carnevale, M. C.; Mahmoudi, H.; Gaeta, S.; Lentini, F.; Drioli, E. *J. Membr. Sci.* **2011**, *376*, 207.
9. Gabelman, A.; Hwang, S. T. *J. Membr. Sci.* **1999**, *159*, 61.
10. Murata, H.; Tomita, Y.; Miyashita, M.; Sakai, K.; Toda, M.; Ohmi, T. *AIChE J.* **1999**, *45*, 681.
11. Zhen, H.; Jang, S. M. J.; Teo, W. K.; Li, K. *J. Appl. Polym. Sci.* **2006**, *99*, 2497.
12. Naim, R.; Ismail, A. F.; Mansourizadeh, A. *J. Membr. Sci.* **2012**, *392*, 29.
13. Ashrafizadeh, S. N.; Khorasani, Z. *Chem. Eng. J.* **2010**, *162*, 242.
14. Wang, K. Y.; Chung, T. S.; Gryta, M. *Chem. Eng. Sci.* **2008**, *63*, 2587.
15. Kim, S.; Chen, L.; Johnson, J. K.; Marand, E. *J. Membr. Sci.* **2007**, *294*, 147.
16. Chung, T. S.; Jiang, L. Y.; Li, Y.; Kulprathipanja, S. *Prog. Polym. Sci.* **2007**, *32*, 483.
17. Vanherck, K.; Aerts, A.; Martens, J.; Vankelecom, I. *Chem. Commun.* **2010**, *46*, 2492.
18. Merkel, T. C.; Freeman, B. D.; Spontak, R. J.; He, Z.; Pinnau, I.; Meakin, P.; Hill, A. *J. Science* **2002**, *296*, 519.
19. Wang, K. Y.; Foo, S. W.; Chung, T. S. *Ind. Eng. Chem. Res.* **2009**, *48*, 4474.
20. Vane, L. M.; Namboodiri, V. V.; Bowen, T. C. *J. Membr. Sci.* **2008**, *308*, 230.
21. Jiang, L. Y.; Chung, T. S.; Kulprathipanja, S. *AIChE J.* **2006**, *52*, 2898.
22. Fang, Z. P.; Xu, Y. Z.; Xu, C. W. *Mater. Sci. Eng.* **2003**, *21*, 279.
23. Yu, L. Y.; Xu, Z. L.; Shen, H. M.; Yang, H. *J. Membr. Sci.* **2009**, *337*, 257.
24. Sukitpaneenit, P.; Chung, T. S. *Ind. Eng. Chem. Res.* **2012**, *51*, 978.
25. Shen, Y.; Lua, A. C. *Chem. Eng. J.* **2012**, *192*, 201.
26. Zhang, Y.; Zhang, G.; Liu, S.; Zhang, C.; Xu, X. *Chem. Eng. J.* **2012**, *204*, 217.
27. Zheng, Y. M.; Zou, S. W.; Nanayakkara, K. G.; Matsuura, T.; Chen, J. P. *J. Membr. Sci.* **2011**, *374*, 1.
28. Yan, L.; Li, Y. S.; Xiang, C. B.; Xianda, S. *J. Membr. Sci.* **2006**, *276*, 162.
29. Jayakumar, O. D.; Mandal, B. P.; Majeed, J.; Lawes, G.; Naik, R.; Tyagi, A. K. *J. Mater. Chem. C* **2013**, *1*, 3710.
30. Bottino, A.; Capannelli, G.; D'asti, V.; Piaggio, P. *Sep. Purif. Technol.* **2001**, *22*, 269.
31. Arthanareeswaran, G.; Sriyamuna Devi, T. K.; Raajenthiren, M. *Sep. Purif. Technol.* **2008**, *64*, 38.
32. Shen, J. N.; Ruan, H. M.; Wu, L. G.; Gao, C. *J. Chem. Eng. J.* **2011**, *168*, 1272.
33. Lua, A. C.; Shen, Y. *Chem. Eng. J.* **2013**, *220*, 441.
34. Shao, J.; Liu, H.; He, Y. *Desalination* **2008**, *234*, 370.
35. Leiknes, T. O.; Semmens, M. *J. Sep. Purif. Technol.* **2001**, *22*, 287.
36. Li, K.; Tan, X. *Chem. Eng. Sci.* **2001**, *56*, 5073.
37. Sun, Y.; Zhang, Z.; Wong, C. P. *J. Colloid Interface Sci.* **2005**, *292*, 436.
38. Chen, Y.; Zhang, Y.; Liu, J.; Zhang, H.; Wang, K. *Chem. Eng. J.* **2012**, *210*, 298.
39. Li, Y. S.; Wang, Y.; Tran, T.; Perkins, A. *Spectrochim. Acta A* **2005**, *61*, 3032.
40. Zhang, Q. G.; Liu, Q. L.; Shi, F. F.; Xiong, Y. *J. Mater. Chem.* **2008**, *18*, 4646.
41. Cong, H.; Radosz, M.; Towler, B. F.; Shen, Y. *Sep. Purif. Technol.* **2007**, *55*, 281.
42. Huang, Z. Q.; Chen, K.; Li, S. N.; Yin, X. T.; Zhang, Z.; Xu, H. T. *J. Membr. Sci.* **2008**, *315*, 164.